

COOLING OF ATOMS

PACS numbers: 32.80.Qk; 37.10.Gh; 37.10.De
DOI: 10.1070/QE2012v042n08ABEH014922

Coherent excitation of the $5D_{5/2}$ level of ultra-cold rubidium atoms with short laser pulses

S.A. Snigirev, A.A. Golovizin, G.A. Vishnyakova, A.V. Akimov, V. N. Sorokin, N.N. Kolachevskii

Abstract. **We demonstrate the use of stimulated Raman adiabatic passage (STIRAP) for population transfer from the ground state to the $5D_{5/2}$ level ($5S_{1/2} \rightarrow 5P_{3/2} \rightarrow 5D_{5/2}$) in laser-cooled ^{87}Rb atoms and examine the influence of the time delay between laser pulses, pulse height, pulse duration and frequency detuning from resonance on the efficiency of Rb atom excitation to the $5D_{5/2}$ level. In our experiments, the pulse duration was varied widely (30–200 ns), which allowed us to assess the effect of spontaneous decay on the population of the $5D_{5/2}$ level (natural lifetime, 300 ns). We performed numerical calculations with allowance for spontaneous decay from the $5P_{3/2}$ and $5D_{5/2}$ levels and compared the results to experimental data, which allowed the population of the $5D_{5/2}$ level to be determined. The maximum population of the $5D_{5/2}$ level in the region under excitation was 80% of the total number of rubidium atoms.**

Keywords: *coherent excitation of atoms, deviation from adiabaticity, magneto-optical trap, rubidium.*

1. Introduction

An accurate experimental determination of atomic level polarisabilities in an electric field remains an important issue in modern spectroscopy because it allows the accuracy of atomic clocks to be improved (see e.g. Refs [1, 2]) and stimulates advances in the theoretical modelling of atoms in an external field. A reliable theoretical calculation of the blackbody radiation shift in an optical clock often determines its ultimate accuracy [3]. To verify theoretical models, it is desirable to be able to compare calculation results with experimentally determined polarisabilities of various atomic levels. The major challenge, from both experimental and theoretical viewpoints, is to determine the polarisability of atomic states that are rather highly excited but do not lie in the Rydberg spectrum (where asymptotic models are well applicable).

In particular, it is of interest to measure the polarisability of the Rb $5D_{3/2,\,5/2}$ levels because available theoretical estimates for these levels depend significantly on the model used [4, 5]. The polarisability of a level can be determined from its Stark shift in an external electric field. To obtain a sufficient luminescence signal, the population of the level should be maximised. Low-lying levels coupled to the ground state by strong dipole transitions are relatively easy to efficiently populate through direct laser excitation. The most challenging problem is to populate short-lived excited states that are not coupled to the ground state by dipole transitions. Among such states are the Rb $5D_{3/2,\,5/2}$ states.

In the framework of a project aimed at studying the Stark shift of the ^{87}Rb $5D_{5/2}$ level, we employed stimulated Raman adiabatic passage (STIRAP) [6, 7], a technique for efficient excitation of atoms by two short laser pulses, demonstrated experimentally in 1990 for transitions between vibrational levels of molecules [8]. It was utilised in the optical spectral region to excite caesium atoms in a beam [9] and was also widely used in a number of other experiments [10–12]. Its main advantage is its high efficiency, up to 100%, in the excitation of atoms to the upper level in three-level systems, which allows this approach to be used e.g. for excitation to Rydberg levels [13], qubit manipulation and quantum state readout [14, 15].

In contrast to previous studies, where the STIRAP technique was employed to populate the rubidium 5D level by short laser pulses [16, 17], we have investigated in detail the nonadiabatic regime, where spontaneous decay has a significant effect on the efficiency of population transfer to the $5D_{5/2}$ level. To this end, the excitation pulse duration was varied from that much shorter than the lifetime of the $5D_{5/2}$ excited level to roughly this lifetime. In the case of the nonadiabatic regime and a limited laser source output power, we searched for optimal relationships between the pulse duration and pulse delay in order to ensure the highest population transfer efficiency. In addition, we calculated excitation processes in the nonadiabatic regime and compared the results to experimental data.

In our experiments, we used a cloud of laser-cooled ^{87}Rb atoms bound in a magneto-optical trap at ~300 μK. At this temperature, the contribution of the Doppler effect on resonance transitions does not exceed 1 MHz, which is less than their natural linewidth. Moreover, the localisation of atoms in a cloud of 0.1 to 1 mm radius allows high excitation intensities to be reached using sources with a relatively low output power, such as semiconductor lasers.

S.A. Snigirev, A.A. Golovizin, G.A. Vishnyakova, V. N. Sorokin, N.N. Kolachevskii P.N. Lebedev Physics Institute, Russian Academy of Sciences, Leninsky prosp. 53, 119991 Moscow, Russia; Moscow Institute of Physics and Technology (State University), Institutskii per. 9, 141700 Dolgoprudnyi, Moscow region, Russia;
e-mail: snigirev.stepan@gmail.com;
A.V. Akimov P.N. Lebedev Physics Institute, Russian Academy of Sciences, Leninsky prosp. 53, 119991 Moscow, Russia; Moscow Institute of Physics and Technology (State University), Institutskii per. 9, 141700 Dolgoprudnyi, Moscow region, Russia; International Center for Quantum Optics and Quantum Technologies, Spasonalivkovskii per. 4, 119991 Moscow, Russia; e-mail: aa@rqc.ru

Received 8 June 2012; revision received 2 July 2012
Kvantovaya Elektronika **42** (8) 714–720 (2012)
Translated by O.M. Tsarev

Using the STIRAP process in the $5S_{1/2} \to 5P_{3/2} \to 5D_{5/2}$ configuration, we investigated the excitation of the upper level in various modes and compared experimental data to theoretical predictions. For the excitation of rubidium with several milliwatts of output power from semiconductor lasers, we found optimal relationships between pulse parameters that maximise the efficiency of population transfer to the $5D_{5/2}$ level. We plan to use the proposed method in subsequent Stark shift measurements for the $5D_{5/2}$ level.

2. Pulsed excitation of levels

Consider a model atom with the allowed electric dipole transitions $|1\rangle \to |2\rangle$ and $|2\rangle \to |3\rangle$ (Fig. 1). The atom interacts with two electromagnetic fields detuned from the resonance frequencies of the $|1\rangle \to |2\rangle$ and $|2\rangle \to |3\rangle$ transitions by δ_1 and δ_2, respectively.

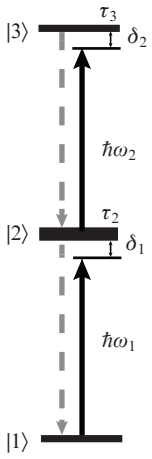

Figure 1. Three-level atom. The $|1\rangle \to |2\rangle$ and $|2\rangle \to |3\rangle$ transitions are dipole-allowed.

In the rotating wave approximation, the Hamiltonian for the interaction of the three-level atom and light has the form

$$H = -\frac{\hbar}{2}\begin{pmatrix} 0 & \Omega_1 & 0 \\ \Omega_1 & \delta_1 & \Omega_2 \\ 0 & \Omega_2 & \delta_1 + \delta_2 \end{pmatrix}, \qquad (1)$$

where $\Omega_1 = E_1 d_{12}/\hbar$ and $\Omega_2 = E_2 d_{23}/\hbar$ are the Rabi frequencies of the corresponding transitions.

Given that there is spontaneous decay from levels $|2\rangle$ and $|3\rangle$, the equation for the density matrix takes the form

$$\frac{\partial \rho}{\partial t} = \frac{1}{\mathrm{i}\hbar}[H, \rho] + \Gamma\rho. \qquad (2)$$

The system of equations for the density matrix components has the form

$$\frac{\mathrm{d}}{\mathrm{d}t}\rho_{11} = \frac{\mathrm{i}}{2}\Omega_1(t)(\rho_{21} - \rho_{12}) + 2\gamma_2\rho_{22},$$

$$\frac{\mathrm{d}}{\mathrm{d}t}\rho_{22} = \frac{\mathrm{i}}{2}\Omega_1(t)(\rho_{12} - \rho_{21}) - 2\gamma_2\rho_{22} + \frac{\mathrm{i}}{2}\Omega_2(t)(\rho_{32} - \rho_{23}) + 2\gamma_3\rho_{33},$$

$$\frac{\mathrm{d}}{\mathrm{d}t}\rho_{33} = \frac{\mathrm{i}}{2}\Omega_2(t)(\rho_{23} - \rho_{32}) - 2\gamma_3\rho_{33}, \qquad (3)$$

$$\frac{\mathrm{d}}{\mathrm{d}t}\rho_{12} = \mathrm{i}\Omega_1(t)(\rho_{22} - \rho_{11}) - \rho_{12}(\gamma_2 + \mathrm{i}\delta_1) - \frac{\mathrm{i}}{2}\Omega_2(t)\rho_{13},$$

$$\frac{\mathrm{d}}{\mathrm{d}t}\rho_{23} = \mathrm{i}\Omega_2(t)(\rho_{33} - \rho_{22}) - \rho_{23}(\gamma_3 + \mathrm{i}\delta_2) + \frac{\mathrm{i}}{2}\Omega_1(t)\rho_{13},$$

$$\frac{\mathrm{d}}{\mathrm{d}t}\rho_{13} = \frac{\mathrm{i}}{2}\Omega_1(t)\rho_{23} + \frac{\mathrm{i}}{2}(\delta_1 + \delta_2)\rho_{13} - \frac{\mathrm{i}}{2}\Omega_2(t)\rho_{12},$$

where $\gamma_2 = 1/\tau_2$ and $\gamma_3 = 1/\tau_3$ are the widths of levels $|2\rangle$ and $|3\rangle$, respectively.

Assume that only level $|1\rangle$ was populated before the fields were applied. Below, we consider two approaches to populating level $|3\rangle$: cascade excitation through an intermediate level and the STIRAP process.

2.1. Cascade excitation

By solving system (3), it is easy to derive a limitation on the population of level $|3\rangle$ in continuous mode, which is 33% (in the limit of high Rabi frequencies). Here and in what follows, cascade excitation is taken to mean pulsed sequential population transfer to level $|2\rangle$ and then $|3\rangle$. In the case of sufficiently long pulses (compared to the lifetimes of the levels), the situation is essentially identical to that under continuous excitation.

A special case is ultra-short pulses with a duration much shorter than the lifetime of level $|2\rangle$. A significant population of level $|3\rangle$ can be reached through the intermediate level $|2\rangle$ by two π-pulses that transfer population from level $|1\rangle$ to $|2\rangle$ (the first pulse) and from $|2\rangle$ to $|3\rangle$ (the second pulse), as illustrated in Figs 2a and 2c. When there is no spontaneous decay, the final population of level $|3\rangle$ is 100% (Fig. 2).

Under real conditions, excitation with π-pulses has a number of drawbacks. If there is spontaneous decay, the durations of both pulses should be much shorter than the lifetimes of states $|2\rangle$ and $|3\rangle$. This condition is often quite hard to satisfy. For example, in our case the lifetime of state $|2\rangle$ (the $5P_{3/2}$ level of the Rb atom) is just 41 ns, which leads to serious difficulties in both generating such short pulses and ensuring that their power density be sufficiently high for maintaining the population oscillation phase.

The most serious difficulties are encountered when levels $|1\rangle$, $|2\rangle$ and $|3\rangle$ have a magnetic structure. The dipole matrix elements for transitions between particular magnetic components may differ, depending on Clebsch–Gordan coefficients, which makes it essentially impossible to simultaneously provide a π-pulse for all the magnetic components and leads to a necessity to monitor the excitation light polarisation. Because of the above drawbacks, this approach is beyond the framework of this paper. A substantial fraction of the above problems can be obviated using the STIRAP process, in which state $|3\rangle$ is populated from state $|1\rangle$ with no population transfer to state $|2\rangle$.

2.2. STIRAP technique

In the case of two-photon resonance ($\delta_1 + \delta_2 = 0$), one of the eigenfunctions of Hamiltonian (1) is the wave function

$$\psi_0(t) = \psi_1 \cos\Theta - \psi_3 \sin\Theta,$$

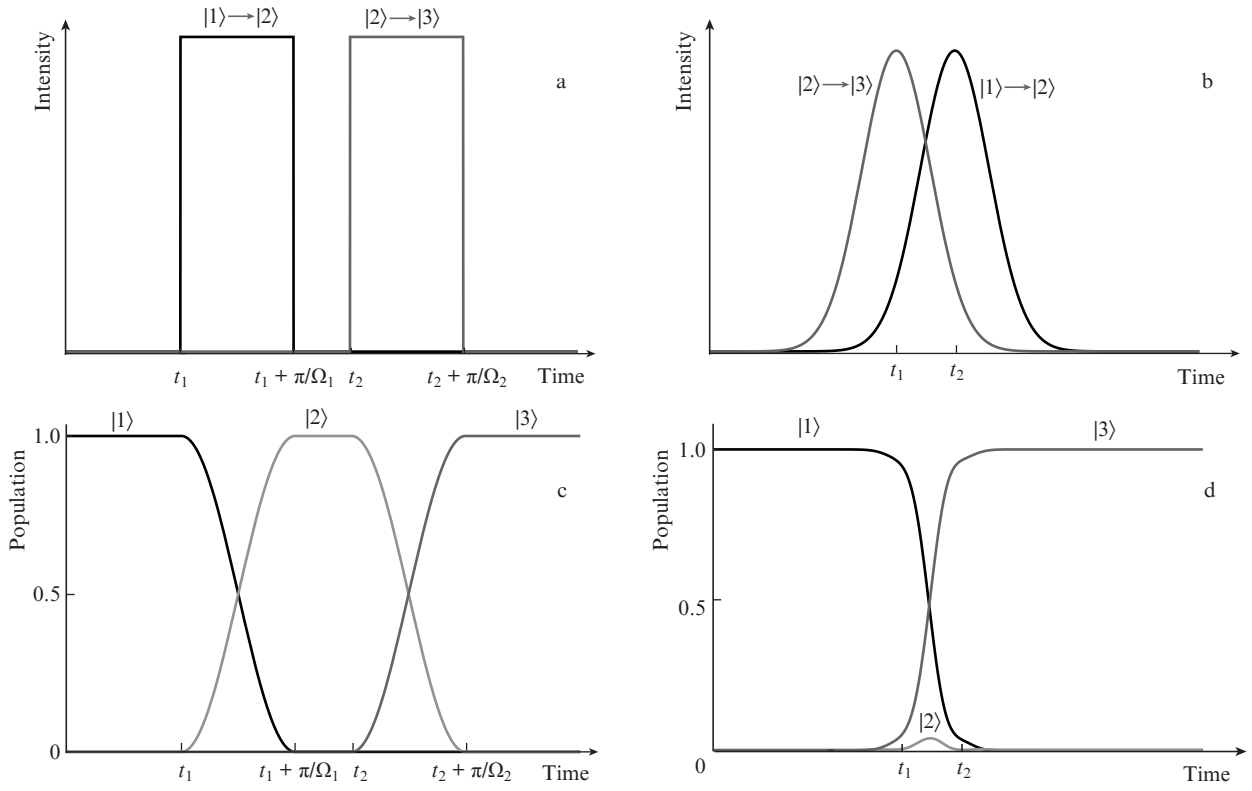

Figure 2. Pulse sequences and population evolution in the system (a, c) under excitation with π-pulses and (b, d) in the STIRAP process.

with zero eigennumber, where $\tan\Theta = \Omega_1(t)/\Omega_2(t)$, and ψ_1 and ψ_3 are the wave functions of states $|1\rangle$ and $|3\rangle$. Note that the wave function of state $|1\rangle$ is missing on the right-hand side. If the atom adiabatically follows state $|\psi_0(t)\rangle$, the population of state $|2\rangle$ is zero at any instant in time, and excitation causes no spontaneous transitions from this level.

At the initial instant t_0, when the population of state $|1\rangle$ is unity, the condition $\Omega_1(t_0) \ll \Omega_2(t_0)$ should be fulfilled, that is, the intensity of the laser pulse that interacts with the $|1\rangle \rightarrow |2\rangle$ transition should be far lower than that of the pulse that interacts with the $|2\rangle \rightarrow |3\rangle$ transition. Further, to adiabatically transfer population to state $|3\rangle$ the intensity of the former pulse should be gradually increased and that of the latter pulse should be decreased until the condition $\Omega_1(t_0) \gg \Omega_2(t_0)$ is fulfilled (Figs 2b, 2d). It is of interest to note that the field that ensures coherence of the empty levels $|2\rangle$ and $|3\rangle$ is applied first. The pulse sequence is thus the inverse of that in the case of excitation with π-pulses.

The STIRAP process is insensitive to the spontaneous decay of state $|2\rangle$. Moreover, there are no stringent requirements for the relationship between the intensity and duration of the laser pulses, which enables high excitation efficiency even at rather long pulse durations and relatively low pulse powers. STIRAP allows one to employ light beams of arbitrary polarisation and excite magnetic sublevels with equal efficiencies because it places no stringent requirements for the correspondence between the pulse shape and the dipole matrix element of the transition.

When the adiabaticity condition is satisfied, the STIRAP process ensures 100% efficiency of population transfer to state $|3\rangle$. Actually, because of the decay from level $|3\rangle$ the excitation efficiency in real systems does not reach 100%. The adiabaticity condition being satisfied means that the decay of the eigenstate corresponding to the wave function ψ_0 is negligible under experimental conditions of interest here. This reduces to the constraint that the frequency of the transition be much higher than the characteristic phase change $|\mathrm{d}\Theta/\mathrm{d}t|$. This condition is well satisfied at high Rabi frequencies and a significant spatial overlap between the beams. This paper presents an experimental study and theoretical analysis of nonadiabatic excitation of state $|3\rangle$ at a limited pulse intensity or at a pulse duration approaching the lifetime of state $|3\rangle$. The system of Eqns (3) was solved numerically with parameters corresponding to experimental conditions. The decay rates $\gamma_{2,3}$ were taken from Ref. [18], and time-dependent Rabi frequencies, $\Omega_{1,2}(t)$, were derived from measured laser pulse profiles. The ionisation of the Rb 5D level by the excitation light was negligible compared to its spontaneous decay because of the large detuning of the laser frequency from the ionisation threshold frequency. The modelling results were compared to experimental data (see Section 4).

3. Experimental

The pulsed excitation process was studied using a cloud of rubidium atoms captured in a magneto-optical trap. The trap was described in detail elsewhere [19]. Figure 3a shows a diagram of the ^{87}Rb levels involved in laser cooling. Cooling was performed on the $5S_{1/2}(F = 2) \rightarrow 5P_{3/2}(F = 3)$ transition using a semiconductor laser (λ = 780.033 nm) based on a DL 7140-2018 laser diode (Sanyo), with an injection amplifier based on a GH0781JA2C diode (Sharp). To return the population to the cooling cycle, we used a repump laser emitting at 780.016 nm. The principal parameters of the atomic cloud during operation of the trap were as follows: the temperature of the atoms, 300 μK; cloud diameter, 500 μm; and number of atoms, 10^6.

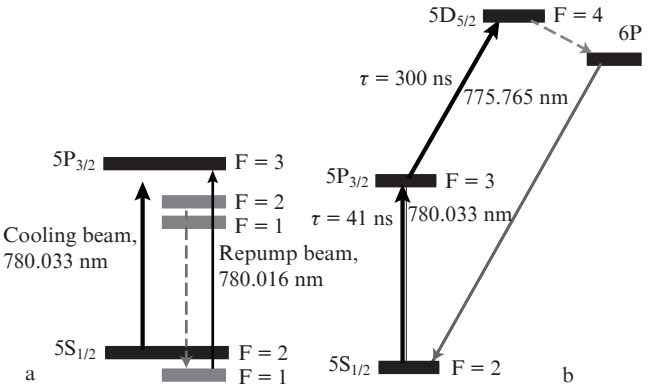

Figure 3. Diagram of the ^{87}Rb levels involved in (a) laser cooling and (b) STIRAP. Also shown is the decay channel for the $5D_{5/2}$ level through 420-nm emission, which was used to detect excited atoms.

The laser-cooled atoms were excited by pulses at 780.033 ($|1\rangle \rightarrow |2\rangle$ transition) and 775.765 nm ($|2\rangle \rightarrow |3\rangle$ transition) through the intermediate level $5P_{3/2}$ (Fig. 3b). The lifetime of the $5P_{3/2}$ level is $\tau_2 = 1/\gamma_2 = 41$ ns, and that of the $5D_{5/2}$ level is $\tau_3 = 1/\gamma_3 = 300$ ns [see Eqns (3)]. The pulse duration was varied from 40 to 200 ns, which allowed us to examine nonadiabatic excitation. The excitation of the atoms to the 5D level was monitored using the 420-nm luminescence due to the $5D_{5/2} \rightarrow 6P \rightarrow 5S_{1/2}$ decay. The decay probability in this channel is 30% (Fig. 3b).

The source of 780.033-nm excitation pulses was the same semiconductor laser as was used for laser cooling because the cooling was stopped at that point in time. The laser frequency varied within 30 MHz. The laser was stabilised relative to the saturated absorption spectrum of a Rb vapour cell. The frequency was tuned to resonance using a Crystal Technology Model 3200 acousto-optic modulator. The 775.765-nm source used was a DL 7140-2018 external cavity laser diode. The frequency was stabilised using the saturated absorption signal from another rubidium vapour cell, heated to 60 °C. To populate the $5P_{3/2}$ level, a time-modulated laser beam stabilised to the $5S_{1/2}(F = 2) \rightarrow 5P_{3/2}(F = 3)$ resonance frequency was launched on the opposite side. In this way, a sub-Doppler signal was generated at the frequency of the $5P_{3/2} \rightarrow 5D_{5/2}$ transition.

Pulses were produced by acousto-optic modulators (Model 3200), which were driven by ZASWA-2-50DR+ switches (Mini-Circuits), with the use of a DG645 delay/pulse generator (Stanford Research Systems). The pulse shape was recorded with a Tektronix DPO 4104 digital oscilloscope and Hamamatsu S5973 photodiode (cutoff frequency, 1 GHz). The signals obtained were subsequently used in numerical simulation. The shortest laser pulse duration obtained in this configuration with no loss in pulse height was 40 ns.

Laser beams differing in wavelength were combined using a polarising cube and then coupled into a single-mode optical fibre, which delivered the radiation to the trap. At the fibre output, the dichromatic beam was focused onto the atomic cloud to a 1/e spot diameter of 1 mm or 100 μm. A typical beam power at the fibre output was several milliwatts. The beam profile was well fitted by a Gaussian.

The total measurement cycle time was 10 μs. The trap beams were switched off for 1 μs, and measurements were made during this time period. Next, the atoms were recaptured and further cooled. The measurement time (1 μs) was divided into intervals: the first 200 ns were used for complete relaxation of the atoms from the 5P level, and the rest of the time was used to excite the 5D level and measure its population. The atomic cloud was exposed to two short pulses whose frequencies were equal to those of the $|2\rangle \rightarrow |3\rangle$ and $|1\rangle \rightarrow |2\rangle$ transitions. The delay between the pulses, $\Delta\tau$, was varied from –200 to +200 ns. The negative delays corresponded to an 'intuitive' pulse sequence, in which the first pulse had the frequency of the $|1\rangle \rightarrow |2\rangle$ transition, and the positive delays corresponded to a 'counterintuitive' pulse sequence, in which the first pulse had the frequency of the $|2\rangle \rightarrow |3\rangle$ transition.

The population of the $5D_{5/2}$ level was assessed from the emission in a narrow band near 420 nm using a Hamamatsu R1925 photomultiplier. The measurement was made with an SR400 photon counter (Stanford Research Systems) over a 1-μs period that included the pulsed excitation cycle. This time window duration was dictated by the $5D \rightarrow 6P \rightarrow 5S$ cascade decay time (300 μs). The typical number of counts at the maximum signal level was 7000 at a total acquisition time of 10 ms (corresponding to 1000 cycles) and was proportional to the population of the 5D level. During that time, there was 150 background counts.

4. Results and discussion

Figure 4 shows typical plots of the 420-nm luminescence signal against pulse delay $\Delta\tau$. The signal has two peaks: the peak at negative time delays corresponds to cascade excitation, and that at positive time delays, to STIRAP excitation. It is seen

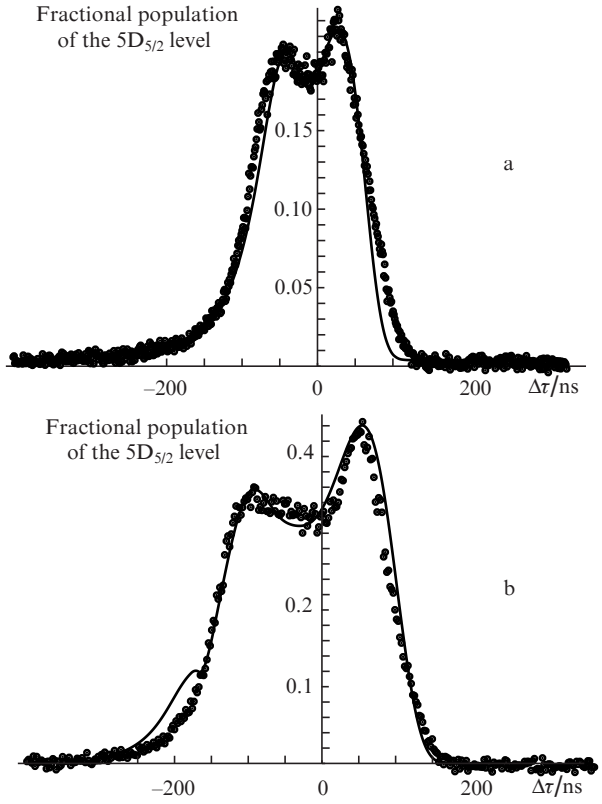

Figure 4. Population of the Rb $5D_{5/2}$ level vs. time delay between the laser pulses, $\Delta\tau$, at pulse durations of (a) 60 and (b) 120 ns. The filled circles represent the experimental data and the solid lines represent a numerical solution to Eqns (3). A 1-mW excitation beam was focused to a spot diameter of 1 mm. The population of the $5D_{5/2}$ level was normalised using simulation results.

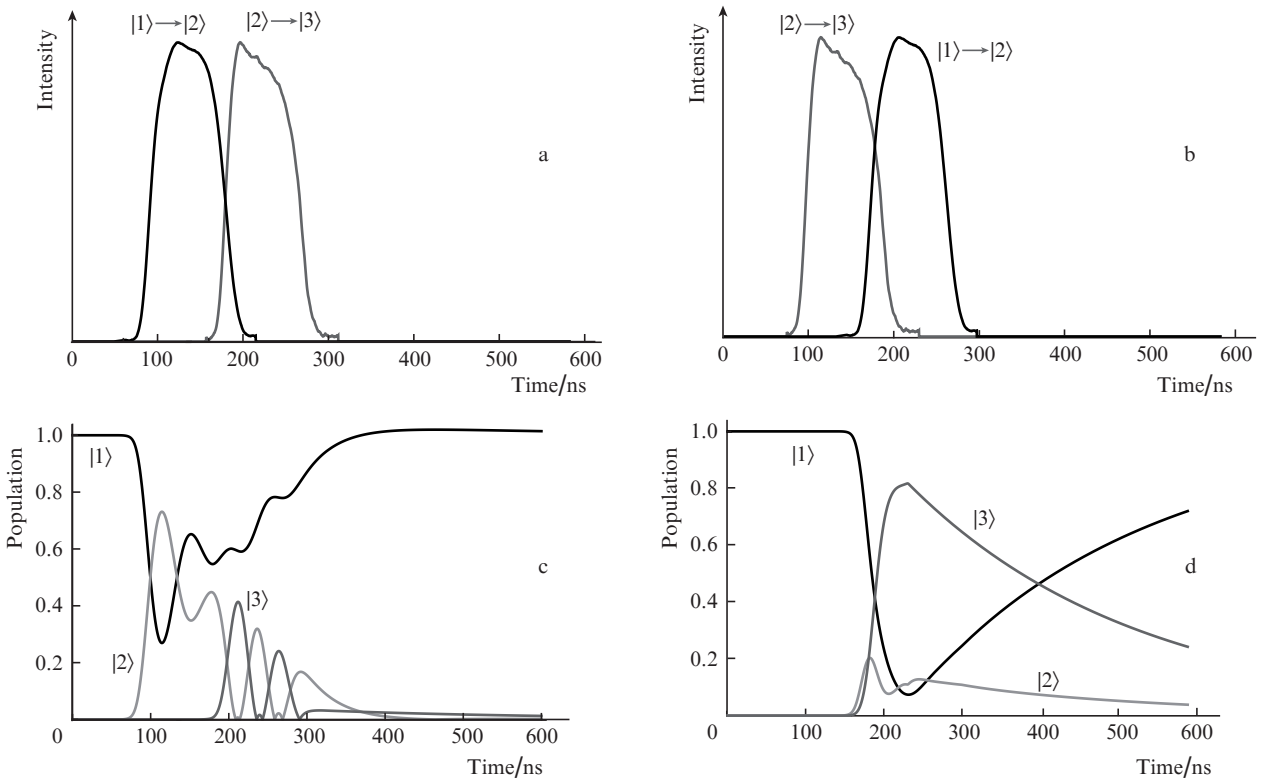

Figure 5. (a, b) Pulse sequences and (c, d) calculated time-dependent level populations for (a, c) cascade and (b, d) STIRAP excitation. The pulse shape used in the simulation corresponds to that in our experiments at a pulse duration of 80 ns. The peak Rabi frequencies for the laser beams are 100 MHz.

that, under the experimental conditions of this study, the STIRAP peak is higher than the cascade excitation peak.

To assess the population of the $5D_{5/2}$ level, we numerically solved the system of Eqns (3). All the atoms were assumed to be under identical excitation conditions: the atomic cloud is optically thin and the laser beam intensity is constant over the cloud size because the beam spot diameter (1 mm) considerably exceeds the cloud size. Figure 5 illustrates the dynamics of the population distribution over levels $|1\rangle$, $|2\rangle$, $|3\rangle$ in two modes: cascade excitation (Figs 5a, 5c) and STIRAP excitation (Figs 5b, 5d).

It is seen that cascade excitation gives rise to Rabi oscillations. In Fig. 5c, the population of level $|3\rangle$ after an excitation cycle is ~5%. Under STIRAP excitation, the population reaches 80% at the instant in time when the pulse resonant to the $|2\rangle \rightarrow |3\rangle$ transition ceases, followed by spontaneous decay. The deviation of excitation efficiency from 100% is caused by the nonadiabaticity of the process (it is seen that the population of the intermediate level does differ from zero), which results from the pulse shape and the spontaneous decay of the excited level. At pulse durations of 80 ns and Rabi frequencies of 100 MHz (16 mW mm^{-2}), about 50% of the loss in excitation efficiency is accounted for by the decay of the $5D_{5/2}$ level; 40%, by the nonoptimal pulse shape; and 10%, by the low beam power.

Analysis of our results indicates that, at pulse durations much shorter than the lifetime of the $5D_{5/2}$ level, increasing the pulse duration allows the adiabaticity of the process to be improved, which has an advantageous effect on excitation efficiency. At the same time, starting at 80 ns an increase in pulse duration causes no increase in excitation efficiency because of the rise in the loss due to the decay of the $5D_{5/2}$ level. At pulse durations over 200 ns, the excitation efficiency decreases because the loss due to the decay of the $5D_{5/2}$ level becomes predominant.

The characteristic population in Fig. 5 is the average population of level $|3\rangle$,

$$p = \int_0^t \rho_{33}(t)\,\mathrm{d}t/\tau_3,$$

which can be assessed from the number of photons detected during the spontaneous decay of the 5D level. The integration was performed over a photon detection time of 1 μs, which far exceeds the lifetime of the 5D level.

Our calculation results agree well with experimental data and can be used to determine the population reached under pulsed excitation. As seen in Fig. 4, the calculated curves agree well with experimental data and allow the population of the $5D_{5/2}$ level to be determined with rather high accuracy. The experimental and theoretical data were compared by finding a calibration coefficient, common to all the measurements, that related the number of counts in the photon counter to the population of the 5D level. Such a coefficient is needed because the absolute intensity at 420 nm is difficult to measure.

Complete automation of the data acquisition and experiment control system allowed us to analyse in detail the excitation process in a wide range of experimental parameters. Figures 6a and 6b show the experimentally determined population of the $5D_{5/2}$ level as a function of pulse duration, delay between the pulses and laser frequency detuning from the resonance frequency of the $5P \rightarrow 5D$ transition. As seen in Fig. 6, the excitation efficiency has a maximum at zero detun-

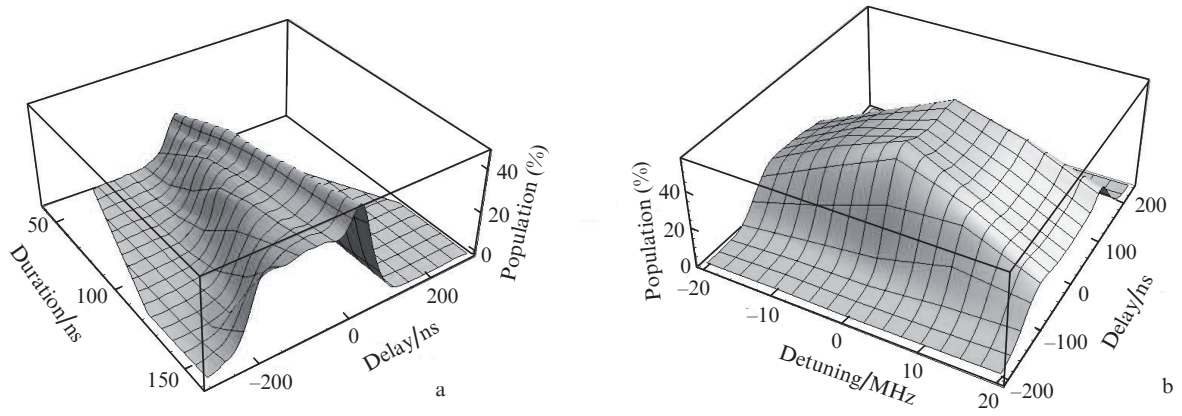

Figure 6. Experimentally determined population of the Rb $5D_{5/2}$ level (a) as a function of laser pulse delay and pulse duration and (b) as a function of laser pulse delay and laser frequency detuning from the resonance frequency of the $5P \rightarrow 5D$ transition (at a pulse duration of 100 ns). The Rabi frequency is 89 MHz for the $5S \rightarrow 5P$ transition and 25 MHz for the $5P \rightarrow 5D$ transition, and the noise is under 5%.

ing from resonance and a pulse delay equal to half the pulse duration. The weak dependence of the excitation efficiency on pulse duration can be understood in terms of the pulse shape in our experiments: the leading and trailing edges of the pulses were essentially independent of pulse duration, in contrast to those of Gaussian pulses. In addition, the population of the level in question was found to be a smooth function of Rabi frequency in the range accessible experimentally (Ω_1 = 5–90 MHz, Ω_2 = 5–25 MHz).

The highest excitation efficiency in our experiments was 40%, which exceeds the cascade excitation efficiency.

Even though the STIRAP excitation efficiency for the 5D level exceeds the cascade excitation efficiency, the upper level population is far from 100%, in contrast to the ideal case. In our experiments, this was primarily due to the limited intensity of the laser beams. To evaluate the maximum achievable excitation efficiency, we carried out an experiment in which the excitation beam was focused to a spot diameter of 100 μm, considerably smaller than the atomic cloud size (Fig. 7a).

When the beam is focused to a small spot, the maximum Rabi frequency is an order of magnitude higher than that in the case of Fig. 4, reaching 890 MHz for the $5S_{1/2} \rightarrow 5P_{3/2}$ transition and 250 MHz for the $5P_{3/2} \rightarrow 5D_{5/2}$ transition. At the same time, the number of atoms interacting with radiation decreases. We numerically modelled the excitation process by solving Eqns (3) with the radial beam intensity profile and atomic density in the cloud taken into account. The modelling results are presented in Fig. 7a and agree well with experimental data. For the atoms situated near the maximum in beam intensity, the population of the 5D level is three times the cloud-averaged population. As in the case of low beam intensities (Fig. 4), the maximum population of the $5D_{5/2}$ level, with an ensemble average of 0.25, is ensured by STIRAP excitation at a pulse delay of 40 ns and pulse duration of 100 ns. The maximum population at the peak intensity is 80%. Thus, provided that a light source of sufficient output power is available, the STIRAP technique indeed enables perfect population transfer from the $5S_{1/2}$ to the $5D_{5/2}$ level of rubidium through the short-lived level $5P_{3/2}$.

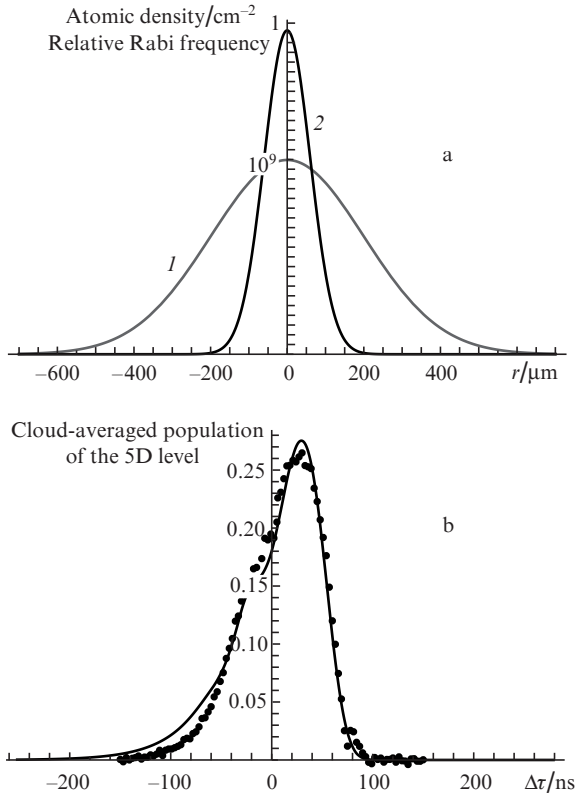

Figure 7. (a) (*1*) Radial profile of the atomic density in the cloud and (*2*) intensity profile of laser pulses focused to a spot diameter of 100 μm (the maximum Rabi frequencies are 890 and 250 MHz). (b) Cloud-averaged population of the 5D level as a function of pulse delay Δτ (solid circles) at a pulse duration of 100 ns (the solid line represents simulation results obtained with the above radial beam profile).

5. Conclusions

We have examined the excitation of the ^{87}Rb $5D_{5/2}$ level in a cloud of laser-cooled atoms by a sequence of two short laser pulses according to the scheme $5S_{1/2} \rightarrow 5P_{3/2} \rightarrow 5D_{5/2}$. The results demonstrate that the STIRAP process ensures a greater population of the $5D_{5/2}$ level than does cascade excitation. When the entire cloud is exposed to pulses that ensure a peak intensity of 2 mW mm^{-2}, the population of the $5D_{5/2}$ level reaches 40% for all the atoms in the cloud. When laser pulses are focused onto a small part of the cloud, the ensem-

ble-average population drops to 25%, but calculations suggest that locally (at the peak intensity) it reaches 80%. Our experimental data are well represented by simulation results obtained by solving Eqns (3) for the density matrix. It is shown that efficient excitation of the $5D_{5/2}$ level is possible by non-Gaussian pulses and at low laser beam intensities (at the level of 1 mW mm^{-2}). The optimal pulse duration that maximises excitation of the $5D_{5/2}$ level under the experimental conditions of this study is 80–150 ns, with a delay between the pulses equal to half the pulse duration. At longer pulse durations, the loss due to the decay of the $5D_{5/2}$ level becomes significant, markedly reducing the excitation efficiency at pulse durations over 200 ns. The proposed approach is planned for use in measurements of the Rb $5D_{5/2}$ level polarisability in an electric field.

Acknowledgements. This work was supported by the Russian Foundation for Basic Research (Grant Nos 12-02-00867a and 11-02-00987a), the RF President's Grants Council (Grant No. MD-669.2011.8) and the Physical Sciences Division of the Russian Academy of Sciences (basic research programme Optical Spectroscopy and Its Applications, 2012–2014).

We are grateful to the students and postgraduates at the Moscow Institute of Physics and Technology who assisted with this study. We are indebted to A. Shavrin and M. Erokhin for the use of their computational resources (about 50 computers) in the numerical modelling of our experiments.

References

1. Ulzega S., Hofer A., Moroshkin P., Weis A. *Eur. Phys. Lett*., **76**, 1074 (2006).
2. Beloy K., Safronova U.I., Derevianko A. *Phys. Rev. Lett.*, **97**, 040801 (2006).
3. Middelmann T., Lisdat C., Falke S., Winfred J.S.R.V., Riehle F., Sterr U. *IEEE Trans. Instrum. Meas*., **60**, 7 (2011).
4. Kamenski A.A., Ovsiannikov V.D. *J. Phys. B. At. Mol. Opt. Phys*., **39**, 2247 (2006).
5. Kondrat'ev D.A., Beigman I.L., Vainshtein L.A. *Kratk. Soobshch. Fiz*., **12**, 3 (2008).
6. Bergmann K., Shore B.W. *Molecular Dynamics and Spectroscopy by Stimulated Emission Pumping* (Singapore: World Scientific, 1995) pp 315–373.
7. Kis Z., Stenholm S. *J. Mod. Opt*., **49**, 111 (2002).
8. Gaubatz U., Rudecki P., Schiemann S., Bergmann K. *J. Chem. Phys*., **92**, 5363 (1990).
9. Pillet P., Valentin C., Yuan R.-L., Yu J. *Phys. Rev. A*, **48**, 845 (1993).
10. Lawall J., Prentiss M. *Phys. Rev. Lett*., **72**, 993 (1994).
11. Goldner L.S., Gerz C., Spreeuw R.J.C., Rolston S.L., Westbrook C.I., Phillips W.D., Marte P., Zoller P. *Phys. Rev. Lett*., **72**, 997 (1994).
12. Weitz M., Young B.C., Chu S. *Phys. Rev. Lett*., **73**, 2563 (1994).
13. Lu X., Sun Y., Metcalf H. *Phys. Rev. A*, **84**, 033402 (2011).
14. Kis Z., Renzoni F. *Phys. Rev. A*, **65**, 032318 (2002).
15. Moller D., Sorensen J.L., Thomsen J.B., Drewsen M. *Phys. Rev. A*, **76**, 062321 (2007).
16. Suptitz W., Duncan B.C., Gould P.L. *J. Opt. Soc. Am. B*, **14**, 5 (1997).
17. Broers B., van Linden van den Heuvell H.B., Noordam L.D. *Phys. Rev. Lett.*, **69**, 2062 (1992).
18. Steck D.A. http://steck.us/alkalidata.
19. Akimov A.V., Tereshchenko E.O., Snigirev S.A., Samokotin A. Yu., Sokolov A.V., Kolachevskii N.N., Sorokin V.N. *Zh. Eksp. Teor. Fiz*., **136** (3), 419 (2009).